OPEN ACCESS
IOP Publishing
Superconductor Science and Technology
Supercond. Sci. Technol. **38** (2025) 065004 (11pp)
https://doi.org/10.1088/1361-6668/add424

Analytical estimates of stress in superconducting dipole magnets for particle accelerators

E Todesco[1,*], P Ferracin[2] and G Vallone[2]

[1] CERN, TE Department CERN, Geneva, Switzerland
[2] Lawrence Berkeley National Laboratory, Berkeley, CA, United States of America

E-mail: Ezio.Todesco@cern.ch

Received 9 December 2023, revised 2 April 2025
Accepted for publication 5 May 2025
Published 23 May 2025

Abstract

For superconducting accelerator magnets based on an overall current density of the order of 500 A mm^{-2}, the electromagnetic forces induce a stress in the winding whose order of magnitude is 100 MPa. This poses special challenges for the mechanical structure, for the insulation, and for the strain induced in the superconductor. The state of stress in a sector coil has two features: an accumulation of the azimuthal component towards the magnet midplane, and an accumulation of radial components towards the structure. In this paper we express the midplane stress as the product of current density, field and aperture radius, plus a shape factor. This equation has been written in similar but not totally equivalent forms, and this form is not only more precise but is also putting in evidence the independent parameters. As known in the literature, for midplane stress higher fields can be mitigated by lower current densities. On the other hand, radial stress scales with the magnetic pressure; here we give a new analytical estimate of the scaling factor, in its dependence on the coil geometry. The used geometrical model is a wedgeless sector coil, that is a good approximation for ratios between coil width and aperture radius up to 2. We present a detailed comparison of the analytical estimates to the finite element results for several cases of coils, and we draw some conclusions on the different magnet designs. Index terms: please choose four to five keywords or phrases in alphabetical order, separated by commas. A hierarchical list of terms is given in the IEEE Taxonomy located online at www.ieee.org/documents/taxonomy_v101.pdf.

Keywords: superconducting dipoles, main magnets for accelerators, magnetic design of superconducting magnets

1. Introduction

The stress induced by the electromagnetic forces in the winding is a critical element of the design of accelerator superconducting magnets. The large current densities (∼500 A mm^{-2} over the insulated winding) and the magnetic fields of ∼10 T, in a magnet aperture of ∼50 mm diameter or larger, can produce a local accumulation of stress well above 100 MPa. For Nb–Ti windings with polyimide insulation, stresses above 150 MPa should be avoided in all phases (assembly, cool-down, powering) not to risk damaging insulation. Nb_3Sn is a brittle conductor, with degradation of critical current in the 100–200 MPa range [1]; for the impregnated winding in the magnet structure dedicated experiments on short model magnets showed first evidence of performance degradation in the 150–200 MPa range [2, 3], with all the caveats associated to the difference between a measured stress in a specific

* Author to whom any correspondence should be addressed.

location, and the stress distributions that can be estimated via a finite element model based on averaged properties and simplifications.

Even though the structure and coil geometries present a level of complexity requiring the use of a finite element code, analytical estimates of the stress induced by electromagnetic forces can be carried out in absence of structure and preload and provide three main advantages:

- Back-of-the-envelope estimates, very useful in the phase of the conceptual design where the trade-off between different parameters (magnet aperture and size, winding thickness and cost of superconductor, current density and protection, …) has to be established;
- Compass to guide magnet design, i.e. to use the equations for finding the good directions to optimize the design (sensitivity analysis);
- Benchmark the magnetic design of the coil, comparing it to analytical estimates.

In this paper we present analytical estimates of the stress in the coil midplane for accelerator dipoles based on 60° sector coils. The main novel elements with respect to the previous works are the following:

- We present the equations for the accumulation of azimuthal stress in the midplane in their natural dependence on current density, field, and aperture, rather than using only two of these quantities, as done in previous literature (section 3). This provides more precise estimates and a better understanding of the parametric dependence. In the midplane and on the inner bore, azimuthal stress is the product of field, current density and aperture radius divided by two.
- We clarify that the integral of the azimuthal forces, a quantity commonly used in the literature, but *a priori* not mathematically justified, corresponds to neglect shear stresses in polar coordinates (section 3.1).
- Radial stress is usually neglected in accelerator dipoles, and scales with the magnetic pressure. Here we present for first time the scaling factor between radial pressure and magnetic pressure (section 4, equations (17) and (18), and figure 5). It turns out that the factor has a peak between 1.5 and 2, and therefore the radial stress is between 50% and twice the magnetic pressure, according to the coil shape. For this reason, it becomes relevant (setting an arbitrary threshold at 150 MPa) for fields of order of 15 T.
- We benchmark both radial and azimuthal analytical estimates with finite element codes in section 5, for a set of accelerator magnets covering a wide range of parameters; this provides for the first time the validity limits of the sector coil model, that should not be used for coil widths larger than aperture diameter.

Equations also give interesting indication/confirmation on the role of grading, of the angles of the layers, and of cable keystoning. The scaling laws allow drawing some conclusions for cases of magnet design, as done in section 6. Three special topics are given in the appendix, namely (i) the analogy between azimuthal stress in dipoles and hoop stress in solenoids, (ii) the required preload to avoid that the coil pole becomes in a state of tension during powering, and (iii) the equations for the azimuthal stress in the quadrupole sector coils.

2. Hypothesis on the model and notations

The scope of this work is to provide analytical estimates of the 2D stress induced by electromagnetic forces, using a model of a dipole coil based on a sector geometry, having a constant current density j. Assuming that the transverse size of the magnet is much smaller than its length, the problem is two-dimensional. The natural coordinate system for this geometry is polar (ρ,θ), see figure 1.

The stress tensor components are the azimuthal $\sigma_{\theta\theta}$, the radial $\sigma_{\rho\rho}$, and the shear $\sigma_{\rho\theta}$ (not shown in figure 1, for sake of clarity), and the equilibrium equations for an infinitesimal volume are [4]

$$\frac{1}{\rho}\frac{\partial}{\partial\rho}\left[\rho\sigma_{\rho\rho}\right]+\frac{1}{\rho}\frac{\partial\sigma_{\rho\theta}}{\partial\theta}-\frac{\sigma_{\theta\theta}}{\rho}+f_\rho=0 \tag{1}$$

$$\frac{1}{\rho}\frac{\partial}{\partial\rho}\left[\rho\sigma_{\rho\theta}\right]+\frac{1}{\rho}\frac{\partial\sigma_{\theta\theta}}{\partial\theta}+\frac{\sigma_{\rho\theta}}{\rho}-f_\theta=0 \tag{2}$$

where the electromagnetic force per unit of volume is the vector product of the current density times the magnetic field

$$\bar{f}=\bar{j}\times\bar{B}. \tag{3}$$

The mechanical structure around the coil has the function of limiting the coil displacements during powering, giving a high rigidity in the radial direction and a coil precompression in the azimuthal one. Here we estimate the stress accumulation in absence of preload, and in presence of an infinitely rigid structure giving a frictionless radial boundary condition. The values provided by these estimates are the inputs for the requirements on the structure rigidity and on the azimuthal preload of the coil.

Given the above hypotheses, the only forces in the problem are the electromagnetic ones, and the peak stress is in the midplane. The azimuthal component $\sigma_{\theta\theta}$ in the midplane has a non zero value on the inner edge of the coil, and then gradually increases inside the coil up to a maximum. The radial component $\sigma_{\rho\rho}$ in the midplane starts from a zero value on the edge of the coil, and increases up to the maximum, corresponding to the region in the coil midplane where the magnetic field is zero. We will give an analytical estimate of the values of these two quantities along the coil midplane in the sections 3 and 4 respectively.

We will integrate the equations for stresses for a sector coil with r as the aperture radius, w as the coil width and j as the overall current density (over the insulated conductor, see figure 2). Note that with respect to the notation used in [5] (a and b for the inner and outer radius of the coil respectively) we prefer to use w and r as in [6]. This provides a better readability and understanding of the equations, since the aperture required by the beam and the coil width needed to produce a given magnetic field are the two independent variables for an

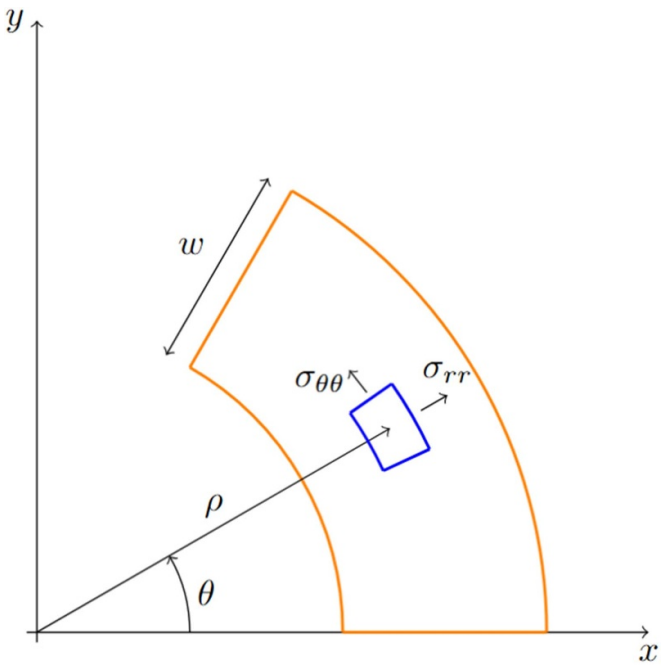

Figure 1. Polar coordinate system for a sector coil of coil width w, with schematic of azimuthal and radial stress in two points of the winding (one quarter shown).

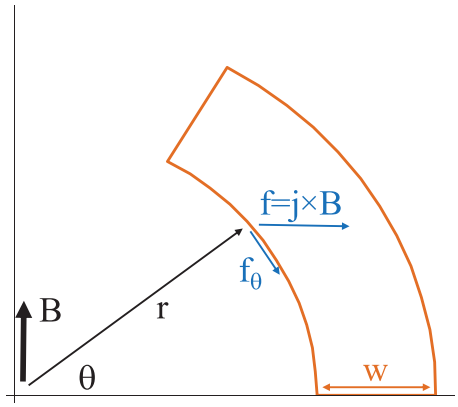

Figure 2. Estimate of the azimuthal stress on the inner edge of the coil (one quarter shown).

accelerator magnet. We have considered a 60° sector coil, that sets to zero the sextupolar component.

3. Analytical estimates of azimuthal stress induced by electromagnetic forces in a sector coil

3.1. Physical meaning of integrating the azimuthal component of electromagnetic forces

In the hypothesis that shear stresses can be neglected equations (1) and (2) become

$$\frac{1}{\rho}\frac{\partial}{\partial\rho}\left[\rho\sigma_{\rho\rho}(\rho,\theta)\right]-\frac{\sigma_{\theta\theta}(\rho,\theta)}{\rho}+f_\rho(\rho,\theta)=0 \tag{4}$$

$$\frac{1}{\rho}\frac{\partial\sigma_{\theta\theta}(\rho,\theta)}{\partial\theta}-f_\theta(\rho,\theta)=0 \tag{5}$$

and integration of the second equation on the midplane $\theta=0$ gives the azimuthal stress on the midplane

$$\sigma_{\theta\theta}(\rho,0)=\rho\int_{\theta_0}^{0}f_\theta(\rho,\theta)\,\mathrm{d}\theta, \tag{6}$$

where θ_0 is the angular width of the sector. This is nothing else than the integral along a circular path of the azimuthal component of the force. This quantity has been widely used in the community to estimate the azimuthal stress in the midplane; however, its physical meaning has always been considered doubtful, since one cannot sum component of forces in a polar system. Here we show that this approximation is correct in the hypothesis that shear stresses in a polar coordinate system can be neglected.

3.2. Integration on the inner bore and relation to magnetic pressure

On the inner radius of the coil the integration is trivial, since one has

$$\sigma_{\theta\theta}(r,0)=jr\int_{\pi/3}^{0}B(r,\theta)\cos\theta d\theta \tag{7}$$

and approximating the field on the inner radius of the coil with the bore field B_I one has

$$\sigma_{\theta\theta}(r,0)\sim jrB_1\int_{\pi/3}^{0}\cos\varphi\,\mathrm{d}\varphi=\frac{jrB_1}{2}. \tag{8}$$

This simple and powerful expression is not known in the literature, and to our knowledge has been first given in [7]. Azimuthal stress in the coil midplane on the inner radius is simply the product of current density, field and aperture radius divided by two. In practical units one has

$$\sigma_{\theta\theta}(r,0)\ [\mathrm{MPa}]\sim\frac{j\left[\mathrm{A/mm^2}\right]r\,[\mathrm{mm}]\,B_1\,[\mathrm{T}]}{2000}. \tag{9}$$

For the LHC dipole [8, 9] having 28 mm aperture radius, 8.3 T field and 360 A mm^{-2} in the inner layer, one gets 42 MPa. Note that for the 5.6 T D1 HL-LHC interaction region magnet [10], the stress is 92 MPa since the aperture radius is 75 mm, and current density is 450 A mm^{-2}. This is putting in evidence that aperture is playing the same role as field in the midplane azimuthal stress. Note also that the presence of iron helps to reduce the stress, since it gives larger fields B without increasing the current densities j.

Recalling that an 60° sector coil has the following dependence between field, current density and coil width (having an iron contribution of Δ_I)

$$B_1=\frac{\sqrt{3}}{\pi}(1+\Delta_I)\,\mu_0 jwj=\frac{\pi B_1}{(1+\Delta_I)\sqrt{3}\mu_0 w} \tag{10}$$

one can rewrite it to put in evidence the magnetic pressure

$$\sigma_{\theta\theta}(r,0) \sim \frac{B_1^2}{2\mu_0}\frac{\pi}{(1+\Delta_I)\sqrt{3}}\frac{r}{w}. \tag{11}$$

A similar expression is found [5] for the average azimuthal stress along the midplane, with the factor $\pi/\sqrt{3} \sim 1.8$ replaced by 4/3. This equation shows that the azimuthal stress in the midplane scales with the magnetic pressure times the ratio between the aperture radius and the coil width. Therefore, for large ratios r/w the azimuthal stress can become much larger than the magnetic pressure. Moreover, as observed in [5, 6] one can reduce the azimuthal stress via a less effective magnet, i.e. increasing the coil width (and reducing the current density).

3.3. Integration for every midplane point in the coil

The full integration based on the field map inside a ironless 60° sector coil with uniform current density is given in [11] and can be written as

$$\sigma_{\theta\theta}(\rho,0) = \frac{1}{2}jrB_1F_\theta(\rho;r,w) \tag{12}$$

where the corrective term when computation is inside the coil is given by

$$F_\theta(\rho;r,w) = \frac{3\rho^2(r+w)-2\rho^3-r^3}{3wr\rho}. \tag{13}$$

Here ρ spans from the aperture radius r to the outer radius of the coil $r+w$, and obviously one has $F_\theta(r;r,w)=1$. This corrective term accounts for the fact that when we enter the coil, the azimuthal component of the stress in the midplane is affected by two opposite effects: the integration length increases since the distance to the center of the magnet becomes larger than r, but the field decreases inside the coil. The first effect is larger, and as soon as you enter the coil, the azimuthal stress increases. The factor depends on the ratio $\xi = w/r$, and its value can be explored via the use of normalized coordinates $\rho' = \rho/r$

$$F_\theta(\rho';1,\xi) = \frac{3\rho'^2(1+\xi)-2\rho'^3-1}{3\xi\rho'} \tag{14}$$

and is shown in figure 3; typically, for thin coils $\xi < 0.5$ (coil widths smaller than half of the magnet aperture radius) the stress increase inside the coil with respect to the value on the edge is quite small (<10%). For very large coils ($\xi > 1$, i.e. coil widths larger than aperture radius) the stress increase is significant. Note that in [6] the same integration is carried out for a cosθ model (i.e. current density varying with the angular coordinate), using equations given in [12] giving the same result: a cosθ model has the same analytical expression of a sector coil for the azimuthal stress in the midplane.

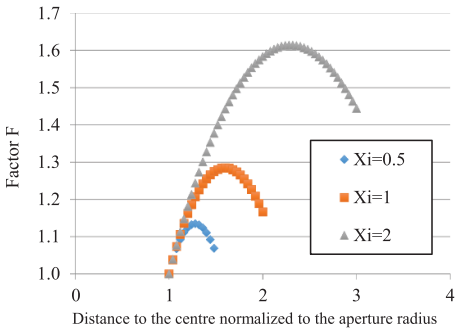

Figure 3. The normalized factor F (see equations (18) and (19)) versus the normalized coordinate ρ/r, for different values of the ratio ξ between coil width and aperture radius.

4. Analytical estimates of radial stress induced by electromagnetic forces in a sector coil

The integration of the component of the radial stress requires the knowledge of the field in the coil along the midplane. A simple hypothesis is that it linearly decreases from B_1 on the inner edge to zero up on the outer edge

$$B(\rho) \sim B_1\left(1-\frac{\rho-r}{cw}\right) \tag{15}$$

as shown in figure 4. Typically, c ranges between 0.6 and 0.8.

Integration of the equation (1) in absence of shear stresses gives

$$\rho\sigma_{\rho\rho}(\rho,0) = \int_\rho^r [\sigma_{\theta\theta}(p,0) - pf_\rho(p,0)]\,\mathrm{d}p \tag{16}$$

and using the hypothesis (equation (15)) for the magnetic field, and the solution (12) for $\sigma_{\theta\theta}$, we obtain

$$\sigma_{\rho\rho}(\rho) = jB_1G_\rho(\rho;c,r,w) \tag{17}$$

with

$$G_\rho = \frac{4(c+3)\rho^3 - 9\rho^2[(c+2)r+3cw] + 6cr^3\ln\left(\frac{\rho}{r}\right) + r^2(5cr+27cw+6r)}{36cw\rho}. \tag{18}$$

It is interesting to rewrite the above expressions in terms of magnetic pressure: since is given by equation (10), one finds

$$\sigma_{\rho\rho}(\rho) = \frac{1}{1+\Delta_I}\frac{B_1^2}{2\mu_0}F_\rho \tag{19}$$

where F_ρ can be written in normalized coordinates as

$$F_\rho = \frac{\pi}{18\sqrt{3}}\frac{1}{c\xi^2\rho'}\Big\{4(c+3)\rho'^3 - 9\rho'^2[(c+2)+3c\xi] + 6c\ln\rho' + (5c+27c\xi+6)\Big\}. \tag{20}$$

The value of this factor in its dependence on the ratio $\xi = w/r$ is given in figure 5 for a coil with $c = 0.65$ and 0.8.

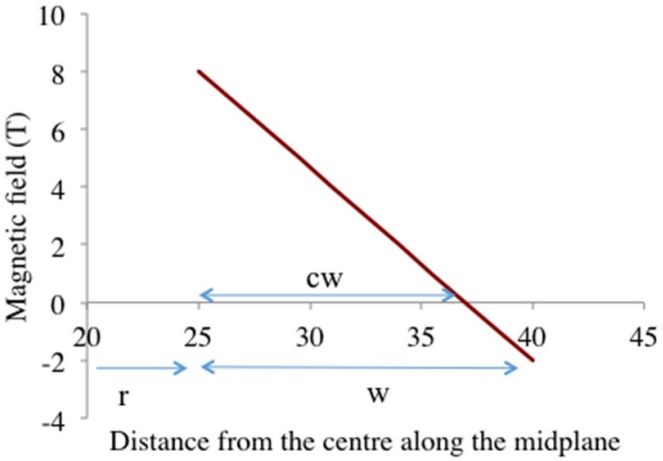

Figure 4. Simplified model for the magnetic field along the midplane in the coil given in equation (15), with $c = 0.8$, for a 25 mm aperture radius dipole giving 8 T field, and 15 mm coil width.

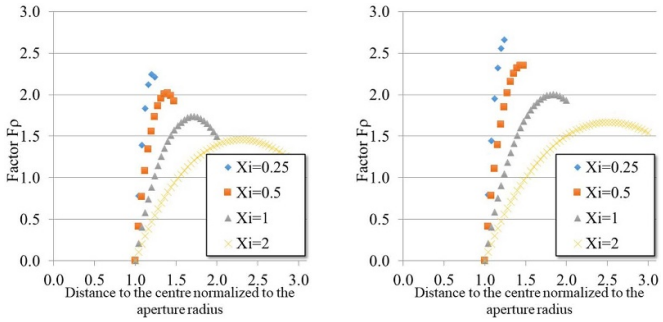

Figure 5. The factor F_{MP} for $c = 0.65$ (left) and $c = 0.8$(right).

This equation shows that radial stress is 50%–100% larger than the magnetic pressure (minus the iron contribution). For small ratio between coil width and aperture radius (0.25–0.5) the radial stress is significantly larger than the magnetic pressure.

Moreover, for a sector coil with 50 mm coil width and 25 mm aperture radius, aiming at 15 T, the radial stress (in absence of iron contribution) is 50% larger than magnetic pressure, i.e. 140 MPa. This is why for accelerator magnets below 15 T usually only the azimuthal stress is considered as relevant, and the impact of the radial stress on the coil performance is neglected.

5. Benchmarking with finite element model

5.1. The finite element model

We consider a two-dimensional finite element model, with plain strain boundary condition, where the coil is made by the actual design with blocks of cables and wedges (i.e. not the equivalent sector coil shown in red in the next figures), and an infinitely rigid structure is present on the outer radius and on the pole of the coil. No friction is assumed for the contact elements between coil and structure. Cable blocks are modeled

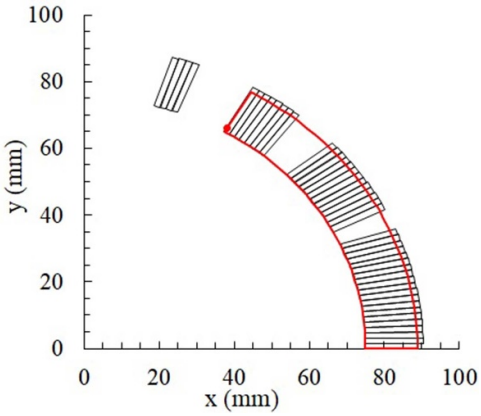

Figure 6. Cross-section of the coil of the HL-LHC D1, and approximation based on 60° sector coil.

with averaged isotropic properties of the conductor plus insulation and resin/voids, whose value have a weak influence on the results. Poisson ratio, that is on the other hand a rather sensitive parameter, is assumed to be 0.3. The model is also used to estimate the magnetic field map, with the iron approximated with a simplified circular geometry. In case of grading, the inner and the outer layers have different current densities, as the insulated cables in the magnet. Typical output are (i) the field map inside the coil (ii) the stress map inside the coil, given in polar coordinates. The sequence of considered cases covers magnets with ratio between coil width and aperture radius from 0.2 (thin one-layer coil) to 2 (thick four layers coils).

5.2. One layer: the separation dipole in the HL-LHC

We start our benchmarking with a 1:5 ratio between coil width and aperture radius, i.e. a coil that is very close to the sector approximation (see figure 6): the best case to use our model. This is the case of the HL-LHC separation dipole D1, having a 15-mm-width coil, and a 75 mm aperture radius to allow the large beam sizes required for HL-LHC [10]. From the geometric point of view, the only main difference between the actual coil and the 60° approximation is the presence of wedges, see figure 6.

This magnet has a bore field of 5.6 T, and a 450 A mm^{-2} overall current density, with a large contribution of the iron (about 60% increase at the nominal current, including iron saturation, i.e. $\Delta_I = 0.60$). The comparison between the equation (12) for azimuthal and the FEM results, and between equation (19) for radial stress and the FEM results is given in figure 7; one can draw the following conclusions:

- The agreement between analytical and numerical estimates is ∼10%.
- The azimuthal stress is 90 MPa, as expected from the analytical expressions; this confirms that the large aperture of the magnet is a driving parameter of the stress, as field and current density.

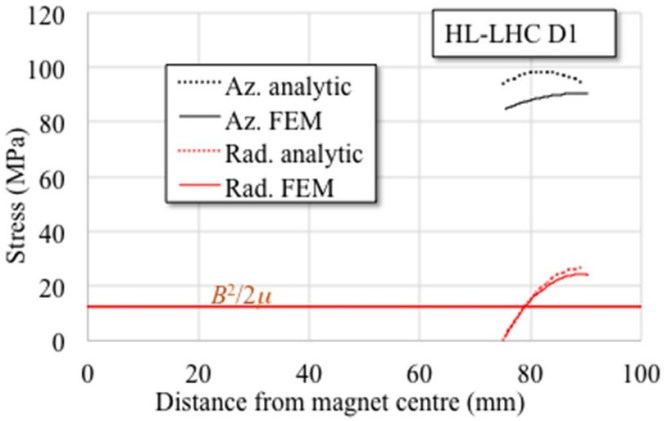

Figure 7. Azimuthal and radial stress along the coil midplane, FEM versus analytical approach, for the HL-LHC D1 magnet.

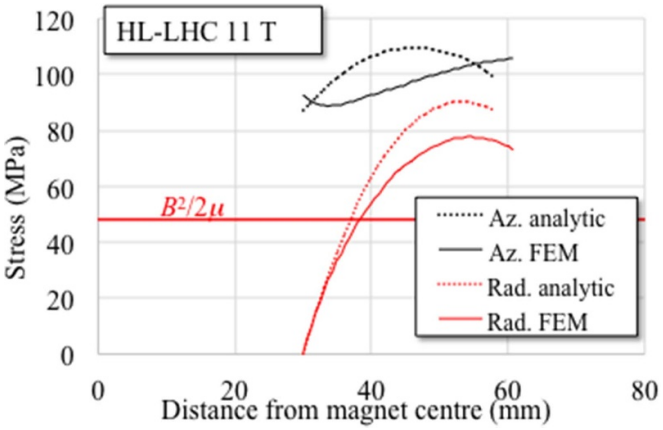

Figure 9. Azimuthal and radial stress along the coil midplane, FEM versus analytical approach, for the 11 T dipole magnet. Two layers: the 11 T dipole in the HL-LHC.

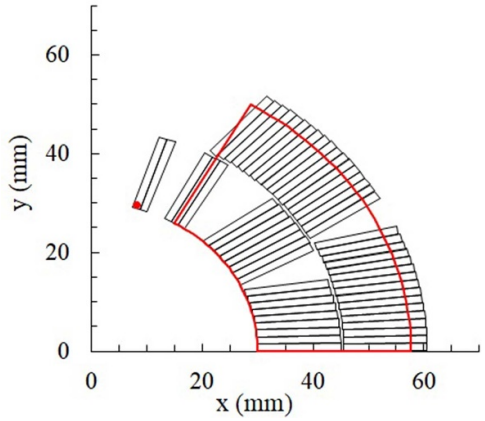

Figure 8. Cross-section of the coil of the 11 T dipole, and approximation based on 60° sector coil.

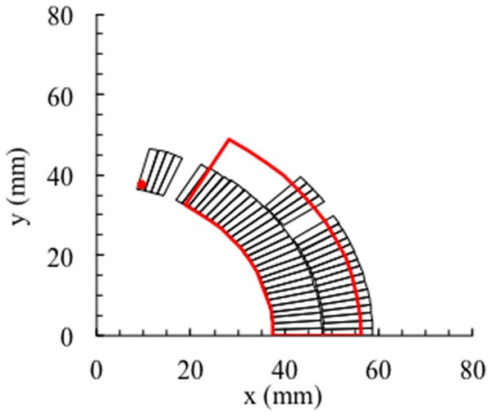

Figure 10. Cross-section of the coil of the HERA main dipole, and approximation based on 60° sector coil.

- The accumulation of radial stress in the midplane is twice larger than the 12 MPa magnetic pressure corresponding to 5.6 T, as expected by the analytical equations.

5.3. Two layers: the HL-LHC 11 T dipole

We move to a 1:1 ratio between coil width and aperture radius, with the double layer coil of the HL-LHC 11 T, see figure 8: the magnet has 11.1 T bore field in a 30 mm aperture radius with a total coil width of 30 mm and an overall current density of 510 A mm^{-2} [13]. The comparison between the analytical model and the FEM is given in figure 9; the agreement is slightly worse than in the previous case, but it is still ∼10%. Note that we deal here with the single aperture case.

5.4. Two layers with angles different from 60°: the HERA main dipole

The HERA main dipole [14] is an interesting case since the angles of the inner and outer layer are considerably different from 60° (see figure 10). The magnet has a 4.5 T field and a 400 A mm^{-2} overall current density: the comparison between analytical and FEM, see figure 11, allows to draw the following conclusions:

- The estimate of the radial stress confirms the 16 MPa found by the FEM, compared to the 9 MPa of the magnetic pressure of a 4.5 T field.
- The analytical estimate of azimuthal stress is 30% lower than the FEM in the inner layer, and 100% larger than the FEM in the outer layer. This is due to the shorter or longer integration path along the arc. This type of coil configuration, as expected by the form of the integral (7), allows to reduce the azimuthal stress in the outer layer at the price of increasing it in the inner layer (as long as the two layers are not impregnated together).

5.5. Two layers, graded coils: the main dipole in the LHC

The study of the main LHC dipole [8, 9] allows to understand the role of grading, i.e. using different current densities in inner and outer layer, see figure 12. It has a 28 mm aperture radius, with a 8.3 T bore field, and 356 A mm^{-2} in the inner layer and 452 A mm^{-2} in the outer layer. Note that we use the single

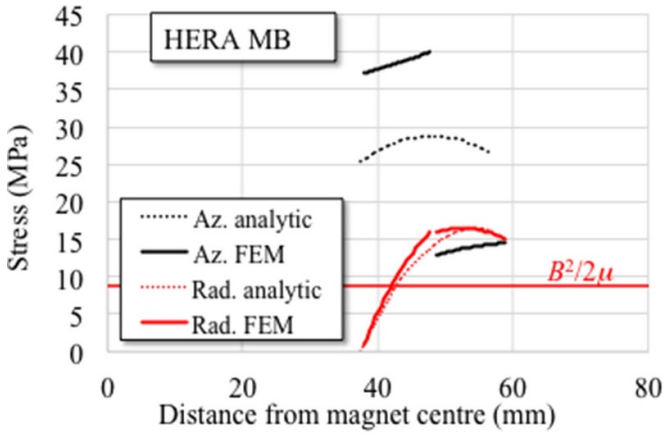

Figure 11. Azimuthal and radial stress along the coil midplane, FEM versus analytical approach, for the HERA main dipole magnet.

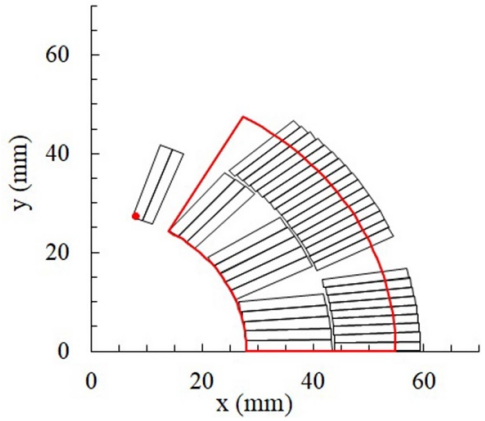

Figure 12. Cross-section of the coil of the LHC main dipole, and approximation based on 60° sector coil.

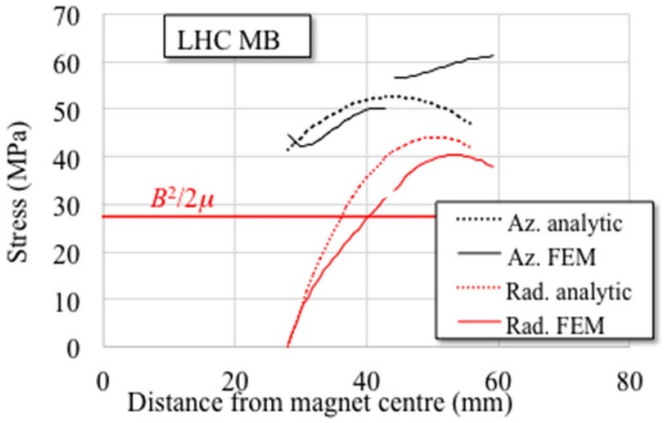

Figure 13. Azimuthal and radial stress along the coil midplane, FEM versus analytical approach, for the LHC main dipole (MB) magnet.

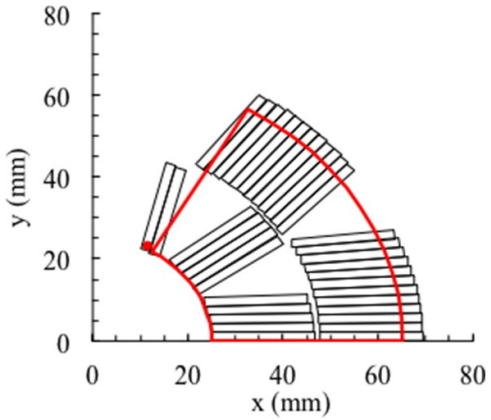

Figure 14. Cross-section of the coil of the FalconD planned dipole, and approximation based on 60° sector coil.

aperture version; to apply our equations we use the current density of the inner layer. Comparison to FEM, see figure 13, gives the following results:

- The FEM computations of the maximum radial stress agree with the analytical equations within 10%.
- The FEM azimuthal stress in the inner layer is also in agreement within 10% to the analytical approach; in the transition from inner to outer layer there is a 20% increase in the FEM, corresponding to the higher current density: as expected, grading increases the azimuthal stress (but not the radial one).

5.6. Two layers: the planned FalconD 12 T dipole

The planned FalconD dipole model [15] is a 12 T, two layers, no graded dipole, with 436 A mm^{-2} overall current density. This is the only case we explore of a magnet not yet built: it is interesting since it has a 1.5:1 ratio between coil width and aperture radius, i.e. 50% larger than the 11 T dipole. This is the largest coil width can be done with two layers, see figure 14.

The discrepancies between sector coil and FEM increase from 10% to 20%, with two opposite effects, see figure 15:

- The FEM shows that when the coil becomes thick with respect to the aperture, the shear stresses in the radial coordinate system are not negligible anymore. This gives an increase of azimuthal stress at the inner radius of the coil from the 65 MPa expected from the simple equation (13) to the 85 MPa found with the FEM.
- The previous effect holds only on the inner radius of the coil: inside the coil, due to the insufficient keystoning of the cable, the analytical estimate of the azimuthal stress in the inner layer rapidly becomes from optimistic to pessimistic, since a large fraction of the sector coil (in red in figure 15) is covered by wedges and not by cable. For this reason, the analytical estimate of the azimuthal stress in the interlayer is 95 MPa, whereas the FEM gives 80 MPa.
- This analytical overestimate of the azimuthal stress also gives an overestimate on the radial stress (100 MPa of peak versus 80 MPa found with the FEM).

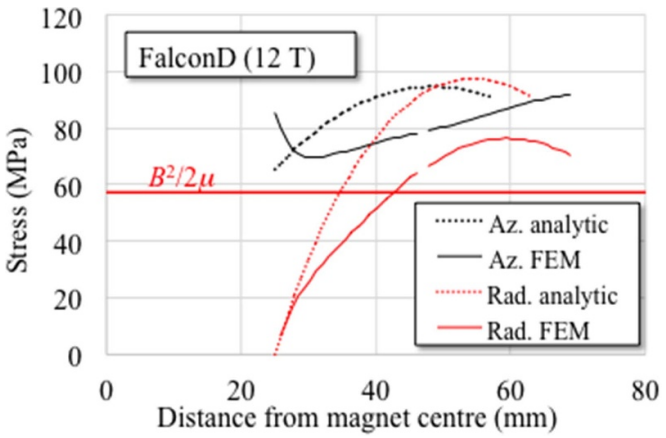

Figure 15. Azimuthal and radial stress along the coil midplane, FEM versus analytical approach, for the FalconD planned dipole magnet.

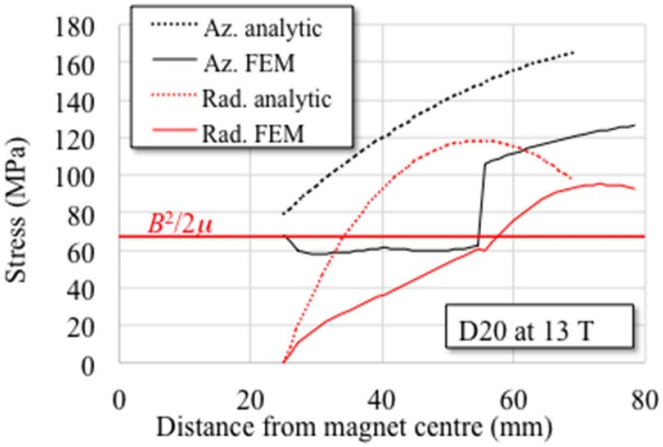

Figure 17. Azimuthal and radial stress along the coil midplane, FEM versus analytical approach, for the D20 dipole model.

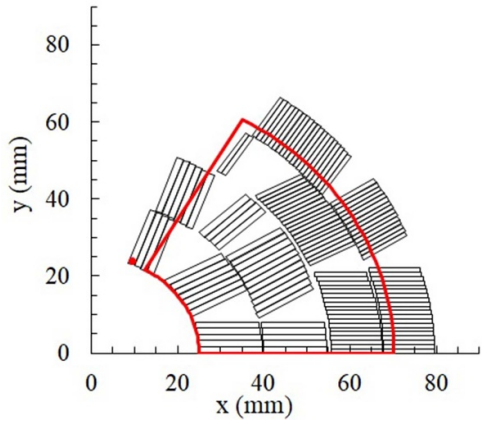

Figure 16. Cross-section of the coil of the D20 dipole model, and approximation based on 60° sector coil.

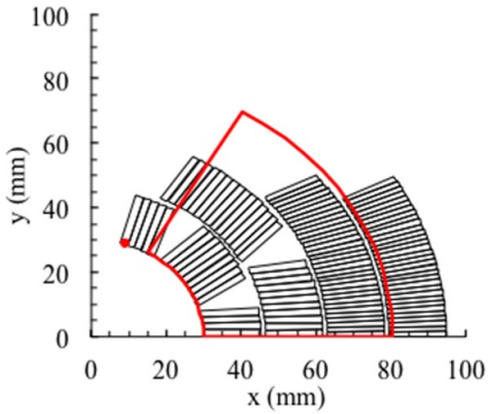

Figure 18. Cross-section of the coil of the MDPCT1 dipole model, and approximation based on 60° sector coil.

5.7. Four layers and graded coils: D20

The D20 dipole model [16] has a ratio 1.8:1 between coil width and aperture radius: therefore, the analytical approach used for the sector model becomes less and less precise, as shear stresses play a more relevant role. This magnet, with 13 T nominal field, has a rather complex four-layer coil with a unprecedented grading, see figure 16: current density in the outer layer is 895 A mm^{-2}, i.e. 80% larger than the 488 A mm^{-2} in the inner layer. Comparison to FEM results is given in figure 17:

- Even though the sector coil approximation becomes less and less precise, the agreement analytical/FEM on the peak values of azimuthal and radial stress is still of the order of 20%, with the FEM values always lower than the analytical values.
- The absence of keystoning confirms the effect already seen in the previous example: the azimuthal stress inside the coil does not increase according to the shape factor in equation (13), since a large part of the sector is not covered by conductor but by wedges. In the case of D20, the analytical approach would forecast an increase from 80 MPa to 140 MPa, whereas the FEM shows that the stress stays around 60 MPa.
- The 80% grading gives a corresponding increase in the azimuthal stress when moving from the inner to the outer layer, as expected.

5.8. Four layers and graded coils: MDPCT1

MDPCT1 [17] is a dipole model with a target field of 15 T: at this field level we see that the radial stress becomes as large as the azimuthal stress. The coil geometry presents the interesting feature of having pole angles far from 60°, as in the HERA dipole design, see figure 18. Aperture radius is 30 mm, the inner coil is made with two layers, each with 15 mm width and 343 A mm^{-2} current density; the outer coil is made of two layers with the same cable width, but with a 468 A mm^{-2} current density.

- The FEM radial stress is within 10% of the analytical equations, and within 140 MPa, see figure 19.
- The azimuthal stress has an interesting pattern: the reduction of the angles in the two outer layers, well below 60°, allows

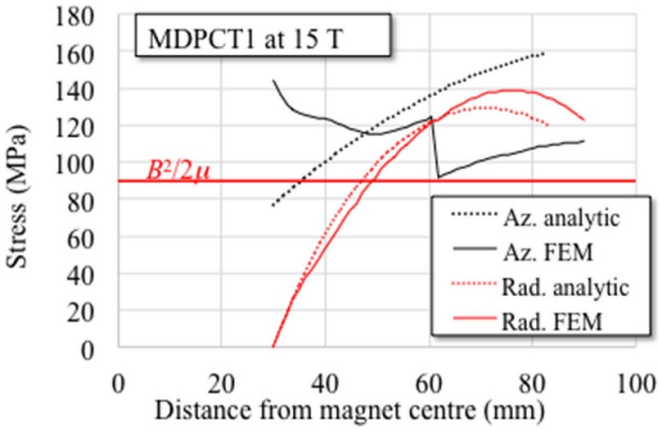

Figure 19. Azimuthal and radial stress along the coil midplane, FEM versus analytical approach, for the MDPCT1 dipole model.

to transform the stress increase due to higher current density to a stress decrease: with this strategy, also the azimuthal stress is below 140 MPa.

- The maximum of the azimuthal stress is on the inner bore, due to presence of bending.

6. Analytical estimates consequences

6.1. Going to high field without exceeding the azimuthal stress limits

A first conclusion can be drawn about the main choice that one has to take when designing a superconducting electromagnet: the balance between current density and coil width to get a given field. Equation (9) shows that higher field magnets can still have a limited azimuthal stress if the current density is reduced. The most effective path to get lower current densities is to use larger coil widths (less effective magnets); here the price to pay is not only the larger mass of conductor, that can be a driving factor of the magnet cost, but also the increase of the stress inside the coil given by the factor F of equation (10). However, we have seen that for very large coil widths this factor overestimates the actual values computed with FEM (see the D20 and the MDPCT1 in sections 5.7 and 5.8).

A second path to lower azimuthal stress is to maximize the iron contribution, that provides more field without increasing the current density. A third path is to use grading (lower current density in the inner layer) as done in the LHC main dipole, in D20 and in MDPCT1. Finally, we pointed out the relevance of the angles of the coil pole: smaller angles greatly reduce the azimuthal stress (as in the outer layer of MDPCT1, see section 5.8), and viceversa (as in the inner layer of HERA dipole, see section 5.2).

6.2. Azimuthal stress and large aperture magnets

A second conclusion concerns the azimuthal stress in the case of large aperture magnets, i.e. magnets with bore diameter larger than the 50–80 mm used in the arcs of colliders from Tevatron to LHC. These magnets can be either in the high luminosity interaction regions, requiring larger apertures due to the large beta functions, or can be dipoles used in test stations for cables (as FrescaII [18] or the planned TFD [19]. In both cases the aperture is in the 100–150 mm diameter range. Since according to equation (8) the stress is proportional to the aperture, these magnets can have an azimuthal stress above 100 MPa even at intermediate fields. For instance, the 5.6 T, 150 mm aperture separation dipole D1 to be installed in the HL-LHC has an azimuthal stress of 110 MPa, ∼50% larger than the 8.3 T, 56 mm aperture LHC arc dipole (see sections 5.1 and 5.4). For this reason, large aperture high field magnets favor the design based on block coils [20], where the issue of the accumulation of the azimuthal prestress on the midplane is removed since (i) the coil geometry is rectangular and (ii) there is an inner structure to intercept the vertical components of the forces, thus avoiding accumulating them on the midplane. Obviously this design has to deal with other difficulties not present in the sector coil, namely the support in the flared ends, the reduction of the aperture due to the inner structure, the singularity in the transition between the lower and the upper deck, etc.

6.3. Radial stress dependence

The analytical approaches show that radial stress is proportional to the bore field and weakly depends on coil parameters as current density or coil pole angles. This means that for a given field the magnet design has very little influence on radial stress.

6.4. When radial stress becomes relevant

The main question we addressed in the radial stress section is: what is the scaling factor between radial stress and magnetic pressure? The analytical estimates and the FEM results show that the radial stress in the midplane is systematically 50% to 100% larger than the magnetic pressure, with 50% to be applied for large coil widths. A 15 T magnet has 90 MPa magnetic pressure, and for a small aperture (25 mm radius) and large coil width (50 mm), the peak radial stress is ∼140 MPa, i.e. approaching the 150 MPa threshold that may require stress management in the radial direction. The dependence on the field in this region is steep: an additional tesla from 15 to 16 T gives an additional stress of 20 MPa.

6.5. Considerations about 20 T magnets

Some conclusions can be finally drawn on 20 T hybrid magnets [21]: firstly, the magnetic pressure of 20 T is 160 MPa and considering the increase due to the factor discussed in the previous section, a structure intercepting radial stress becomes mandatory. Secondly, an HTS insert giving a total bore field of 20 T, in a 50 mm aperture diameter and working at 400 A mm^{-2} has an accumulated stress on the bore of already 100 MPa (see equation (8)). This value can only increase inside the coil, or due to effects as discussed in 5.6 and 5.8, and therefore it

appears to be at the limit of the design values: for this reason, current densities much higher than 400 A mm^{-2} or apertures larger than 50 mm are not viable without a azimuthal stress management, unless the HTS can be made resistant up to 200 MPa stresses.

7. Conclusions

In this paper we extensively discussed analytical estimates of the stress induced by electromagnetic forces in a winding of superconducting accelerator magnets, in the case of an infinitely rigid structure, absence of preload and in a coil based on a sector geometry with a ratio between coil width and aperture diameter not larger than one (or ratio between coil width and aperture radius not larger than two). These hypotheses and boundary conditions are discussed in section 2.

For the accumulation of azimuthal stress, discussed in section 3, we recalled the previous approaches in the literature, pointing out that this stress does not scale with magnetic pressure and that large fields can be compensated by lower current densities, making the magnet less effective but allowing to go well above 10 T. We point out that the most effective way to express the azimuthal stress is a product of field, current density and aperture (equations (8), (12) and (13)), that are the independent variables of the magnet design. This allows pointing out two relevant features: (i) azimuthal stress is proportional to the aperture, and therefore for very large apertures it can become a critical aspect, and (ii) iron contribution can play a relevant role to reduce the accumulation of azimuthal stress, since it produces additional field with the same current density.

The radial stress, discussed in section 4, is an issue that is usually considered as less relevant in accelerator dipole magnets. We show that it basically scales with the magnetic pressure and is 50% to 100% larger than the magnetic pressure, the second values corresponding to thinner coils. This implies that for 20 T a radial stress management is mandatory.

We benchmark the analytical equations with seven magnet cross-sections, with quite different shapes and aspect ratios, finding in the cases of thinner coils a 10% agreement, and 20% for the thicker coils. The benchmark also allows to point out the influence of grading, coil angles, and coil shapes as discussed in section 5.

Data availability statement

The data cannot be made publicly available upon publication because they are not available in a format that is sufficiently accessible or reusable by other researchers. The data that support the findings of this study are available upon reasonable request from the authors.

Acknowledgment

We wish to acknowledge A Yamamoto for stimulating the discussion on the relation between azimuthal stress and magnetic pressure during the lectures given during the first wave of the COVID-19 pandemic. D Tommasini pointed us the analogy between azimuthal stress in dipoles and hoop stress in solenoids. Finally, thanks to A Milanese for reading this manuscript and giving significant feedback on the discussion on preload estimates of appendix B.

Appendix A. Hoop stress in solenoids

The winding in the solenoid of aperture r, thickness w and having a magnetic field B is subjected to a horizontal force equal to

$$F_x = 2\int_0^{\pi/2} \frac{B^2}{2\mu_0} r\cos\theta \mathrm{d}\theta = 2r\frac{B^2}{2\mu_0}. \tag{21}$$

If the winding is not supported by an external structure, a stress is induced in the winding

$$\sigma_{\theta\theta} = \frac{F_x}{2w} = \frac{r}{w}\frac{B^2}{2\mu_0} \tag{22}$$

and it is usually called hoop stress. Note that this expression has the same dependence on variables as the azimuthal stress in the dipoles, given in equation (11). The main difference with respect to a dipole is that the Hoop stress is a uniform tension, independent of the angle, whereas in the dipole the stress depends on the angle, with compression in the midplane and tension in the pole. This makes the dipoles much more challenging than the solenoids in terms of mechanics.

Appendix B. Preload estimates

In order to avoid the state of tension in the pole at nominal powering, an azimuthal preload is imposed; this preload displaces the coil pole of the same quantity that is given by electromagnetic forces. At nominal current, the preload effect disappears and one is left with the distribution of the stress that has been discussed in this paper. Therefore, the preload does not sum up to the electromagnetic forces at nominal current, but simply disappears.

A significant quantity is the ratio between the required preload (after assembly, at cryogenic conditions) and the accumulation of stress in the midplane of the electromagnetic forces. This ratio can be estimated as

$$\frac{\int_{\frac{\pi}{3}}^{0} \theta f(\theta)\,\mathrm{d}\theta}{\int_{\frac{\pi}{3}}^{0} f(\theta)\,\mathrm{d}\theta} \tag{23}$$

where f is the force density along the angle. If the electromagnetic forces were all acting on the pole, this ratio would be one, i.e. one would need to apply a preload equal to the accumulation of stress in the midplane. If the forces were uniformly distributed along the angle, the needed preload would be half of the accumulation of the stress on the midplane. In our case, the azimuthal force is zero in the midplane, since all the component is radial, and increases towards the pole. Assuming a linear dependence one finds

$$\frac{\int_{\frac{\pi}{3}}^{0}\theta^2 \mathrm{d}\theta}{\int_{\frac{\pi}{3}}^{0}\theta \mathrm{d}\theta}=\frac{2}{3} \tag{24}$$

and if we assume a $\sin\theta$ dependence one finds

$$\frac{\int_{\frac{\pi}{3}}^{0}\theta\cos\theta \mathrm{d}\theta}{\int_{\frac{\pi}{3}}^{0}\cos\theta \mathrm{d}\theta}=\sqrt{3}-\frac{\pi}{3}\sim 0.68 \tag{25}$$

therefore the required preload (after cool-down) is 65%–70% of the accumulated azimuthal stress in the midplane. When a full model, including structure and coil properties is used, the required preload turns out to be not far from 100% of the electromagnetic forces.

Appendix C. Azimuthal stress in quadrupoles

We give for completeness also the equations for a quadrupole winding based on 30° sector coil, given in [7]. The azimuthal stress on the inner radius of the coil is given by

$$\sigma_{\theta\theta}(r,0)=jr^2G\int_{\frac{\pi}{6}}^{0}\cos 2\theta \mathrm{d}\theta=\frac{jr^2G}{4} \tag{26}$$

and the shape factor is

$$\sigma_{\theta\theta}(\rho,0)=\frac{jr^2G}{4}F(\rho;r,w) \tag{27}$$

with

$$F(\rho;r,w)=\frac{\rho^4-r^4+4\rho^4\ln\frac{r+w}{\rho}}{4r^2\rho^2\ln\left(1+\frac{w}{r}\right)} \tag{28}$$

ORCID iDs

E Todesco https://orcid.org/0000-0001-5518-4191
P Ferracin https://orcid.org/0000-0003-0415-8895
G Vallone https://orcid.org/0000-0003-0716-8116

References

[1] Ekin J J W 1987 Effect of transverse compressive stress on the critical current and upper critical field of Nb_3Sn *J. Appl. Phys.* **62** 4829–34
[2] Felice H *et al* 2011 Performance of a Nb_3Sn quadrupole under high stress *IEEE Trans. Appl. Supercond.* **21** 1849–53
[3] Mangiarotti F *et al* 2022 Performance of a MQXF Nb_3Sn quadrupole magnets under different stress *IEEE Trans. Appl. Supercond.* **32** 4007106
[4] Timoshenko S P and Goodier J N 2008 *Theory of Elasticity* (McGraw-Hill)
[5] Wilson M N 1983 *Superconducting Magnets* (Oxford Science Publications)
[6] Caspi S and Ferracin P 2005 Limits of Nb_3Sn accelerator magnets *Particle Accelerator Conf.* pp 107–11
[7] Todesco E *et al* 2021 Review of the HL-LHC interaction region magnets towards series production *Supercond. Sci. Technol.* **34** 054501
[8] Perin R 1998 *Encyclopedia of Applied Superconductivity* (IOP) pp 919–50
[9] Rossi L *et al* 2003 The LHC main dipoles and quadrupoles toward series production *IEEE Trans. Appl. Supercond.* **13** 1221–8
[10] Nakamoto T *et al* 2015 Model magnet development of D1 beam separation dipole for the HL-LHC upgrade *IEEE Trans. Appl. Supercond.* **25** 4000505
[11] Fessia P, Regis F and Todesco E 2009 Parametric analysis of forces and stresses in superconducting quadrupoles sector windings *IEEE Trans. Appl. Supercond.* **19** 1203–7
[12] Meuser R 1978 Magnetic field for a thick cos-nθ winding *Engineering Note M5254* (Lawrence Berkeley National Lab)
[13] Karppinen M *et al* 2012 Design of 11 T twin aperture Nb_3Sn dipole demonstrator magnet for LHC upgrades *IEEE Trans. Appl. Supercond.* **22** 4901504
[14] Wolff S 1988 Superconducting HERA magnets *IEEE Trans. Magn.* **24** 719–22
[15] Valente R, Bellomo G, Fabbricatore P, Farinon S, Mariotto S, Pampaloni A, Prioli M, Sorbi M and Statera M 2020 Electromagnetic and mechanical study for the Nb_3Sn cos-theta dipole model for the FCC *IEEE Trans. Appl. Supercond.* **30** 4001905
[16] Dell'Orco D, Scanlan R and Taylor C E 1993 Design of the Nb_3Sn dipole D20 *IEEE Trans. Appl. Supercond.* **3** 82–86
[17] Novitski I, Andreev N, Barzi E, Carmichael J, Kashikhin V V, Turrioni D, Yu M and Zlobin A V 2016 Development of a 15 T Nb_3Sn accelerator dipole demonstrator at Fermilab *IEEE Trans. Appl. Supercond.* **26** 4001007
[18] Milanese A, Devaux M, Durante M, Manil P, Perez J C, Rifflet J M, de Rijk G and Rondeaux F 2012 Design of the EuCARD high field model dipole Fresca2 *IEEE Trans. Appl.* **22** 4002604
[19] Vallone G *et al* 2021 Magnetic and mechanical analysis of a large aperture 15 T cable test facility dipole magnet *IEEE Trans. Appl. Supercond.* **31** 9500406
[20] Sabbi G L *et al* 2005 Design of HD2: a 15 tesla Nb3Sn dipole with a 35 mm bore *IEEE Trans. Appl. Supercond.* **15** 1128–31
[21] Ferracin P *et al* 2023 Conceptual design of 20 T hybrid accelerator dipole magnets *IEEE Trans. Appl. Supercond.* **33** 4002007